arXiv:cond-mat/0308228v1 [cond-mat.supr-con] 12 Aug 2003

Topological doping of repulsive Hubbard models

A. Kesting[1,2] and C. Timm[2]

[1]*Institute for Economics and Traffic, Dresden University of Technology, Andreas-Schubert-Strasse 23, D-01062 Dresden, Germany**

[2]*Institut für Theoretische Physik, Freie Universität Berlin, Arnimallee 14, D-14195 Berlin, Germany*

(Dated: August 12, 2003)

The spin configuration induced by single holes and hole pairs doped into stoichiometric, antiferromagnetic cuprates is considered. Unrestricted Hartree-Fock calculations for the three-band Hubbard model are employed to study spin-polaron and vortex-like (meron) solutions. Meron solutions for a single hole are found to be metastable with higher energy than spin polarons. We observe that the meron solution shifts from site-centered to bond-centered as the interaction is increased. Meron-antimeron solutions for hole pairs are found to be unstable. The results are in agreement with earlier findings for the one-band Hubbard model. However, we find that the Hubbard interaction of the one-band model has to be chosen similar to the one of the three-band model to obtain comparable results, not of the order of the charge-transfer gap, as previously expected.

PACS numbers: 74.72.-h,75.50.Ee,71.27.+a

I. INTRODUCTION

Superconductivity appears in cuprates upon introduction of electrons or holes into the insulating, antiferromagnetic parent compounds. These are insulators due to the strong electron-electron interactions, which lead to a Mott-Hubbard splitting of the bands. Upon doping with holes, the antiferromagnetic order is lost at about 2% holes per copper atom and the system becomes superconducting at a somewhat higher doping level. The doping of Mott-Hubbard insulators has been studied quite extensively. Nevertheless there is still no agreement on what happens when a few electrons or holes are introduced.

From experiments as well as from band-structure calculations it is known that the undoped compounds have one hole in each Cu d-shell, whereas the oxygen-dominated bands are completely filled. Consequently, the Cu ions carry spins 1/2, which order antiferromagnetically due to superexchange. Electron and hole doping are qualitatively different: Electrons mostly fill the Cu hole so that the local spin vanishes. Holes predominantly reside in the planar oxygen orbitals, introducing another spin 1/2. This physics can be modelled by the three-band Hubbard Hamiltonian

$$\mathcal{H}_{3\mathrm{B}} = \epsilon_d \sum_{i\sigma} d^\dagger_{i\sigma}\, d_{i\sigma} + \epsilon_p \sum_{j\sigma} p^\dagger_{j\sigma}\, p_{j\sigma} + t^{\pm}_{pd} \sum_{\langle ij\rangle\sigma} \left(p^\dagger_{j\sigma} d_{i\sigma} + \mathrm{h.c.} \right) + U_d \sum_i n^d_{i\uparrow} n^d_{i\downarrow}, \tag{1}$$

where $d^\dagger_{i\sigma}\,(p^\dagger_{j\sigma})$ is the creation operator of an electron in a $3\mathrm{d}_{x^2-y^2}$ ($2\mathrm{p}_x$, $2\mathrm{p}_y$) orbital at site i (j) and $n^d_{i\sigma} = d^\dagger_{i\sigma}\, d_{i\sigma}$ is the corresponding density operator. The parameters ϵ_d, ϵ_p denote onsite energies. The hopping amplitude $t^{\pm}_{pd}$ between nearest-neighbor copper and oxygen sites $\langle ij\rangle$ changes sign due to the two possibilities of overlap, *e.g.*, positive (negative) for the bonds pointing from a Cu site in the positive (negative) x and y directions. Finally, U_d is the onsite Coulomb interaction for two electrons on the same Cu site with opposite spins.

The Coulomb interaction U_p between oxygen electrons is irrelevant for the case of one or two holes, since the probability of two holes sitting on the same oxygen ion is extremely low. Furthermore, the hybridization between the oxygen orbitals is omitted as the hopping t_{pd} is the dominant process. Furthermore we neglect the Coulomb interaction between Cu and O electrons.

Electron and hole doping also have rather different experimental consequences: Antiferromagnetic order is destroyed by only $x \sim 0.02$ holes per Cu, whereas it survives on the electron-doped side up to $x \sim 0.14$. This asymmetry is easily understood: Electrons dilute the antiferromagnet, which perturbs the order relatively weakly. On the other hand, holes introduce extra oxygen spins, which couple antiferromagnetically to both their neighboring Cu spins, resulting in a strong *ferromagnetic* coupling between those spins [1]. This ferromagnetic bond strongly frustrates the antiferromagnet, leading to its rapid destruction [1, 2, 3]. This picture is supported by experiments on cuprates doped with nonmagnetic impurities such as zinc [4, 5]. They dilute the spin system similarly to electron doping, leading to a large critical concentration for the destruction of antiferromagnetic order [5], which is essentially a percolation transition [6].

The qualitative difference between electron and hole doping suggests that a small number of charge carriers doped into the parent compounds should also behave quite differently. Indeed, several authors propose that hole doping leads to the appearance of nontrivial structures of the surrounding Cu spins, such as dipolar configurations [1, 7], vortices or merons [8, 9, 10], skyrmions [11, 12, 13], and domain walls or stripes [8, 9, 14, 15, 16].

*Electronic address: kesting@vwisb7.vkw.tu-dresden.de

This should be contrasted with a spin-polaron configuration, where the spins in the vicinity of the hole might be reduced or even inverted in sign but are still collinear. Timm and Bennemann [2] have proposed a mechanism for the rapid destruction of antiferromagnetic order in the hole-doped regime that relies on the formation of merons in the staggered magnetization upon doping. We here use the term "meron" to refer to a topological defect in the easy-plane Heisenberg model. It is very similar to a vortex in the XY model, but the order parameter may rotate out of the easy plane close to the defect center in a "lotus flower" configuration. The easy-plane anisotropy is caused by the Dzyaloshinskii-Moriya interaction [17, 18], resulting from buckling of the CuO_2 planes and spin-orbit coupling. For energy reasons, merons are expected to be created as meron-antimeron pairs. It is suggested that merons appear since each hole introduces a ferromagnetic Cu-Cu bond, leading to frustration, which can be reduced by forming merons centered on each such bond [2]. This mechanism only works for hole doping, not for electron doping, in agreement with the pronounced asymmetry of the phase diagram.

The question of the existence of meron-antimeron pairs in the ground state has been studied with various approaches [8, 9, 10]. The present situation is not satisfactory, since unrestricted Hartree-Fock calculations for the one-band Hubbard model have found meron-antimeron pair solutions, but never as the ground state [8]. On the other hand, Hartree-Fock calculations have been performed for the three-band model [19, 20], but meron-antimeron pairs have not been considered.

The one-band Hubbard model can be derived from the three-band model, Eq. (1), as an effective low-energy model [21]. The one-band model is defined by the Hamiltonian

$$\mathcal{H}_{1\mathrm{B}} = -t \sum_{\langle ij\rangle,\sigma} \left(c^\dagger_{i\sigma} c_{j\sigma} + \mathrm{h.c.}\right) + U \sum_i c^\dagger_{i\uparrow} c_{i\uparrow} c^\dagger_{i\downarrow} c_{i\downarrow}. \quad (2)$$

In the undoped three-band model the Fermi energy lies between an occupied oxygen-type band and the unoccupied upper Hubbard band. The charge-transfer gap between them is mimicked by the Mott-Hubbard gap of the one-band model and the onsite interaction U of the one-band model must be chosen accordingly [22, 23]. However, this derivation [21] of the one-band model assumes a polaron-like configuration for a doped hole and would not work if meron-antimeron pairs were the true ground state.

On the other hand, a slave-boson approach did find meron-antimeron pairs as the ground state for two holes, again in the one-band model [9]. This approach goes beyond the Hartree-Fock approximation (HFA) and leads to lower variational ground-state energies. Furthermore, in a one-band spin-flux model Berciu and John [10] also find meron-antimeron pairs as the ground state, employing the configuration-interaction (CI) method, which also goes beyond Hartree-Fock theory. Both approaches have not yet been applied to the three-band model. The question appears to be open.

In the present paper we consider the three-band Hubbard model within the HFA. In Sec. II we briefly outline the theory. In Sec. III we compare the results with Hartree-Fock calculations for the one-band model for larger system sizes than studied previously. We study the stability of spin-plasmon and meron solutions for a single hole and, in particular, of meron-antimeron solutions for two holes. We also consider changes in the meron structure as a function of the interaction strength.

II. THEORY

Since it is mostly standard, we can be brief in describing our implementation of the unrestricted Hartree-Fock approximation [24]. We here do this for the three-band Hubbard model. The HFA reduces the many-body problem to a set of single-electron problems by decoupling the interaction, in our case in the particle-hole channel. To include transverse spin degrees of freedom we decouple on the level of creation and annihilation operators,

$$\begin{aligned} &U_d \sum_i d^\dagger_{i\uparrow} d_{i\uparrow}\, d^\dagger_{i\downarrow} d_{i\downarrow} \\ &\cong U_d \sum_i \left(d^\dagger_{i\uparrow}, d^\dagger_{i\downarrow}\right) \begin{pmatrix} \langle n^d_{i\downarrow}\rangle & -\langle S^-_i\rangle \\ -\langle S^+_i\rangle & \langle n^d_{i\uparrow}\rangle \end{pmatrix} \begin{pmatrix} d_{i\uparrow} \\ d_{i\downarrow} \end{pmatrix} - E_0, \end{aligned} \quad (3)$$

with the spin-flip operators $S^+ = S^x + iS^y = d^\dagger_\uparrow d_\downarrow$ and $S^- = S^x - iS^y = d^\dagger_\downarrow d_\uparrow$ and the constant energy shift

$$E_0 = U_d \sum_i \left(\frac{1}{4}\langle\, n^d_i\rangle^2 - \langle S^z_i\rangle^2 - \langle S^x_i\rangle^2 - \langle S^y_i\rangle^2\right). \quad (4)$$

After decoupling the interaction, the many-particle ground state $|\Psi\rangle$ for $T = 0$ in the HFA is constructed by creating N_e electrons in the lowest-energy single-particle states out of the vacuum $|0\rangle$,

$$|\,\Psi\,\rangle = \prod_{n=1}^{N_e} a^\dagger_n\, |\,0\,\rangle. \quad (5)$$

The single-particle states are given in terms of wave functions ϕ_n by

$$a^\dagger_n = \sum_{i\sigma} \phi_n(i,\sigma)\, c^\dagger_{i\sigma}, \quad (6)$$

where the sum over i runs over all relevant Cu $\mathrm{d}_{x^2-y^2}$ and oxygen p_x and p_y orbitals, and $c^\dagger_{i\sigma}$ creates an electron in orbital i.

The Hartree-Fock eigenequations are derived by minimizing the expectation value to the total energy in the state $|\Psi\rangle$ with the $\phi_n(i,\sigma)$ as variational parameters. For

the n-th state with spin $\sigma =\uparrow,\downarrow$ at the Cu site i the equation is of the form

$$E_n\,\phi_n(i,\sigma) = -t_{pd}^{\pm}\sum_{j\in V_i}\phi_n(j,\sigma) + \sum_{\nu}\left(\left(\frac{U_d}{2}+\epsilon_d\right)\langle n_i^d\rangle\delta_{\sigma\nu} - U_d\boldsymbol{\sigma}_{\sigma\nu}\langle\mathbf{S}_i\rangle\right)\phi_n(i,\nu). \tag{7}$$

The notation $j \in V_i$ means that the sum is performed over the sites j which are nearest neighbors of site i. $\boldsymbol{\sigma} = (\sigma^x, \sigma^y, \sigma^z)$ is the vector of Pauli matrices and σ^0 is the unit matrix. The local Hartree-Fock fields of the charge and spin density,

$$\langle n_i^d\rangle = \langle\Psi|\sum_{\mu\nu} d_{i\mu}^\dagger\sigma_{\mu\nu}^0 d_{i\nu}|\Psi\rangle = \sum_{n\sigma}|\phi_n(i,\sigma)|^2, \tag{8}$$

$$\langle\mathbf{S}_i\rangle = \frac{1}{2}\langle\Psi|\sum_{\mu\nu} d_{i\mu}^\dagger\boldsymbol{\sigma}_{\mu\nu} d_{i\nu}|\Psi\rangle = \frac{1}{2}\sum_{n\mu\nu}\phi_n^*(i,\mu)\boldsymbol{\sigma}_{\mu\nu}\phi_n(i,\nu) \tag{9}$$

are computed self-consistently. The sum over n is performed for the N_e electrons in the system. The terms for the oxygen sites j are of an analogous form. Finally, the Hartree-Fock ground-state energy is given by the sum of the eigenvalues E_n for occupied states,

$$E_N = \sum_{n=1}^{N_e} E_n - E_0. \tag{10}$$

We solve the Hartree-Fock equations (7) by iteration, which requires a numerical diagonalization at each step. Self-consistency is assumed when the difference in all spin and charge components is less than $\epsilon \simeq 10^{-5}$. Typically, the charge distribution converges very rapidly to the self-consistent value, while the spin configuration needs a lot more iteration steps. The number of steps depends strongly on the initial configuration and the boundary conditions.

III. RESULTS AND DISCUSSION

In the present section we examine the Hartree-Fock solutions for the three-band Hubbard model for one and two holes [24]. The results are compared with corresponding ones for the one-band model. The calculations have been carried out for a square lattice with up to 14×14 unit cells for the three-band model as well as for the one-band model. We have treated periodic as well as open boundary conditions (BC). The latter disturb the elementary cells at the edge of the lattice in the three-band case. We have studied edges of alternating copper and oxygen ions but also edges made up entirely of oxygen ions. Finite size effects are stronger for open BC, as expected, but are neglectible for the lattice sizes used here. Relevant parameters in the three-band model are (i) the hopping t_{pd}, (ii) the Coulomb interaction U_d for copper sites and (iii) the band gap $\Delta = \epsilon_p - \epsilon_d$ between the oxygen and copper orbitals. A Coulomb interaction between oxygen electrons and a non-zero oxygen-oxygen hopping amplitude do not change the solutions qualitatively and are neglected in the present study. A band gap $\Delta > 0$ in combination with $U_d > \Delta$ implies that holes preferentially occupy oxygen orbitals as observed in experiments. In this regime the occupied oxygen states and the empty copper states in the upper Hubbard band are separated by a charge-transfer gap, which is given by $U_d - \Delta$. For the calculations we have used the parameters taken from Ref. [25],

$$t_{pd} = 1\,\text{eV}, \quad U_d = 8\,\text{eV}, \quad \Delta = 5\,\text{eV}. \tag{11}$$

The results for the three-band model are compared to corresponding Hartree-Fock results for the one-band Hubbard model [8] with $t = 1$ eV and U in the range from 5 to 8 eV.

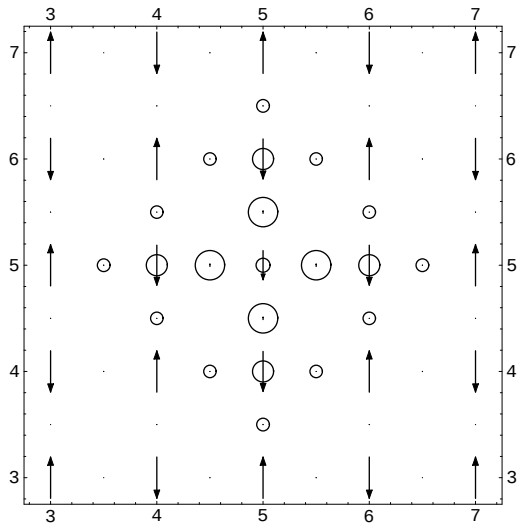


FIG. 1: Self-consistent Hartree-Fock solution of the three-band Hubbard model for one hole. The figure shows part of a 10×10 lattice with the spin and relative charge density indicated for each atomic site by the arrows and circles, respectively. The reduced copper spin at point $(5, 5)$ forms a spin polaron with its four nearest copper neighbors. The charge is mainly distributed over the four oxygen neighbors.

A. Single-hole solutions

For a single hole we find a spin-polaron configuration as the self-consistent solution of the HFA for open as well as periodic boundary conditions, see Fig. 1. In its center a reduced copper spin (of modulus 0.55 in units where the fully polarized state corresponds to unity vs. an average order parameter of 0.78) is pointing in the same direction as its four nearest copper neighbors, *e.g.*, a ferromagnetic "microdomain" is formed. The charge

is mainly distributed over the four oxygen neighbors of the central copper ion. Small magnetic moments at the oxygen sites are induced, which are oriented oppositely to the copper spins. This result is consistent with the overcompensation of the antiferromagnetic superexchange by an effective ferromagnetic Cu-Cu coupling for all values of $U_d > \Delta$, supporting the picture of Aharony *et al.* [1].

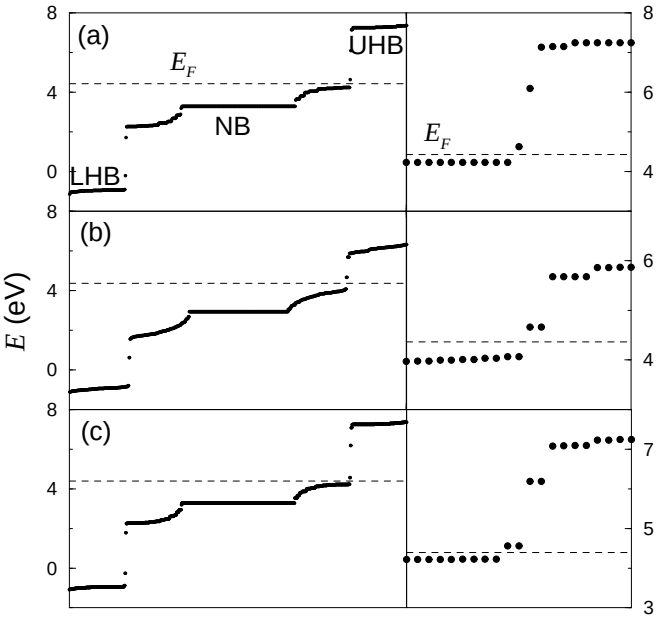


FIG. 2: One-particle energy spectra for self-consistent solutions of the HFA. LHB and NB denote the occupied lower Hubbard and non-bonding bands, respectively. UHB denotes the unoccupied upper Hubbard band [22, 23]. (a) Spectrum for the spin-polaron solution of Fig. 1. (b) Spectrum for the meron solution of Fig. 3(a). (c) Spectrum for the solution of Fig. 6. The right-hand-side figures are enlargements of the regions close to the Fermi energy.

In the one-particle spectrum of Fig. 2(a) *two* states appear in the gap due to the interaction. One is split off from the occupied oxygen-dominated band but is now empty due to the extra hole. This is the Zhang-Rice singlet [21]. The other state originates from the unoccupied upper Hubbard band. The first unoccupied state is to about 75% localized on oxygen sites emphasizing the oxygen character of doped holes [26].

It is worth considering the limit of strong interaction $U_d/t_{pd} \gg 1$ studied by Zhang and Rice [21]. For $U_d = 50\,\mathrm{eV}$, $\Delta = 25\,\mathrm{eV}$ we find a polaron solution similar to Fig. 1, but with the copper spin moment in the polaron center hardly reduced (to 0.99) and the charge mainly (to 80%) localized on its four oxygen neighbors. These four ions together carry a spin moment of -0.79. Thus in the HFA the central copper spin forms a singlet with its four oxygen neighbors, as predicted [21].

It is instructive to compare the results with the one-band Hubbard model, for which the polaron configuration is also a self-consistent solution in the HFA [8]. For an intermediate interaction of $U \approx 5 \ldots 8\,\mathrm{eV}$ the charge distribution and the spin moment at the polaron center are of the same order of magnitude as in the three-band case so that in this respect the one-band model indeed mimicks the three-band physics. However, it is surprising that we find this relation for values of U for the one-band model similar to $U_d = 8\mathrm{eV}$ and *not* to the charge-transfer gap $U_d - \Delta = 3\,\mathrm{eV}$, as we would have expected [22, 23]. On the contratry, for $U \lesssim 3\mathrm{eV}$ we find the diagonal cigar-shaped configuration predicted in Refs. [27, 28] without any inverted Cu spin [24]. We suggest that U is of the order of U_d since the local moment is dominated by the interaction in the copper d orbital and is only marginally affected by the hybridization with oxygen orbitals.

We now turn to meron configurations for a single doped hole. We start the HFA with a coplanar vortex configuration. Site-centered Merons turn out to be stable Hartree-Fock solutions for $U_d \lesssim 7\,\mathrm{eV}$. Because of the non-vanishing winding number only open boundary conditions are possible. In Fig. 3(a) a site-centered meron solution for $U_d = 7\,\mathrm{eV}$ is shown for a lattice with edges of alternating copper and oxygen ions. But there is no qualitative difference to lattices with edges made up entirely of oxygen ions. Increasing U_d shifts the center of the meron first in the direction of a plaquette and then onto a bond, see Figs. 3(b) and (c). In addition, a tendency towards ferromagnetic alignment, *i.e.*, formation of a spin polaron, is observed. These results correspond to the one-band solutions for $U \gtrsim 8\,\mathrm{eV}$, in which the spin in the meron center is no longer suppressed and shows a tendency towards formation of a ferromagnetic microdomain. Note that again U has to be chosen similar to U_d and not to the charge-transfer gap to obtain this result. To exhibit the transition from site- to bond-centered merons more quantitatively, we plot in Fig. 4 the average $\langle \mathbf{S} \rangle^2$ at the site $i = (6, 6)$ for the three-band solution and the corresponding quantity for the one-band model. For a site-centered meron this number is negligible due to symmetry.

For the one-band model we have compared the energies of polaron and meron solutions for a single hole by considering their respective formation energies [29]. As expected, the meron energy is higher than the energy of the spin polaron and diverges logarithmically with system size. However, the iteration process of the HFA turns out to be unable to change the winding number. Adding small random numbers during the iteration process makes it converge to a spin-polaron configuration. Thus a meron is a *metastable* solution.

In the one-particle spectrum for the meron solution with $U_d = 7\,\mathrm{eV}$, Fig. 2(b), two discrete, degenerate hole states appear: one from the filled oxygen-dominated non-bonding band and the other from the unoccupied upper Hubbard-band. The states are degenerate because an additional electron can be introduced either with spin up or spin down. The same holds for the one-band model. A mirror image of these degenerate states appears in the gap between the occupied bands.

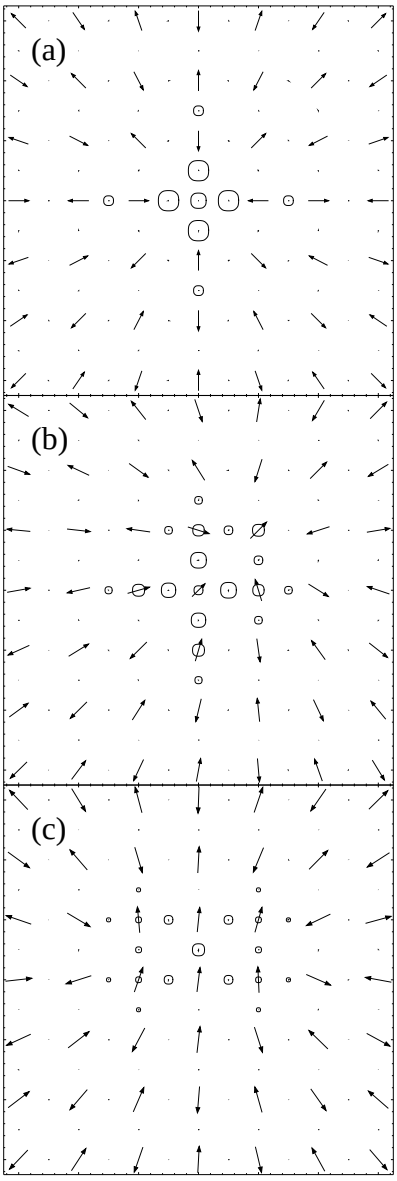


FIG. 3: Selfconsistent Hartree-Fock solutions with (a) $U_d = 7\,\mathrm{eV}$, (b) $U_d = 8\,\mathrm{eV}$ and (c) $U_d = 10\,\mathrm{eV}$ on an 11×11 lattice. For $U_d \leq 7\,\mathrm{eV}$ site-centered merons are stable solutions of the HFA. Increasing U_d shifts the center of meron but preserve the winding number of the initial configuration.

B. Two-holes solutions

We now turn to a system doped with *two* holes to investigate possible meron-antimeron solutions. As initial configurations we consider pairs of bond-centered as well as plaquette-centered defects, see Fig. 5, and both open and periodic BC. We find that these configurations are not stable under the HFA iteration. This result holds for all parameter sets we have investigated. Instead, the system develops into a polaron-type spin configuration, the detailed structure of which depends on the choice of BC. For example, Fig. 6 shows the solution for the

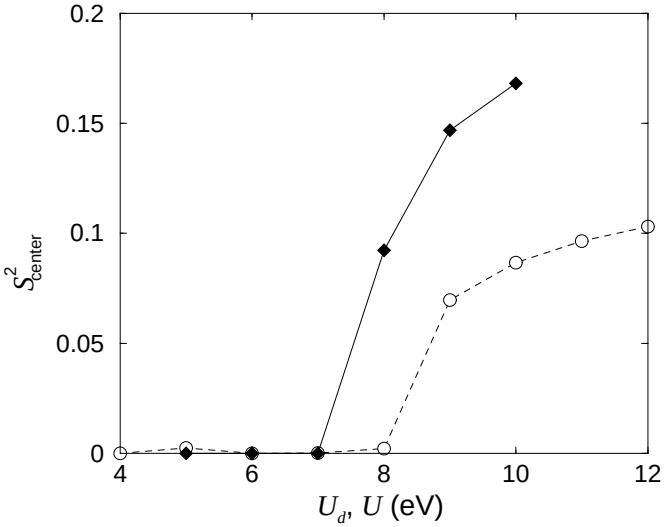


FIG. 4: The average value $\langle \mathbf{S} \rangle^2$ at the site closest to the meron center as a function of the interaction U for the one-band model and U_d for the three-band model. For a site-centered meron, $\langle \mathbf{S} \rangle^2$ is negligible due to symmetry. A non-vanishing value corresponds to a qualitative change in the spin texture, see Fig.3.

bond-centered initial configuration and periodic BC on a 14×14 lattice. We find two spin polarons with antiferromagnetically aligned center spins. The polaron centers are localized on neighboring copper sites. At the oxygen sites small magnetic moments are induced which are oriented in antiparallel to the copper spins.

The origin of the instability of meron-antimeron solutions is their higher energy and their vanishing winding number. The latter means that they can be destroyed during the HFA iteration since no high energy barrier has to be overcome. Since for large separations $\mathbf{R}$ of meron and antimeron the interaction increases logarithmically with $\mathbf{R}$, the energy of the meron-antimeron solution will eventually become larger than the spin-polaron energy. However, our results indicate that this is also the case at the smallest separations.

Again, similar results are obtained for the one-band model. Bond-centered as well as plaquette-centered meron-antimeron pairs as initial configurations develop into spin polaron solutions as shown earlier by Vergés *et al.* [8]. In contrast, Seibold [9] has found a stable solution in the one-band model using a slave-boson approximation beyond Hartree-Fock.

In Fig. 2(c) the spectrum of the discussed double-polaron solution is shown. For each doped hole one state splits off from the occupied non-bonding band and another from the unoccupied upper Hubbard band. The first two hole states are localized to about 80% on oxygen sites. Further, the states are energetically degenerate reflecting the symmetry of the solution under inversion in the center of the bond between $(7, 6)$ and $(7, 7)$ in Fig. 6 and simultaneous spin inversion.

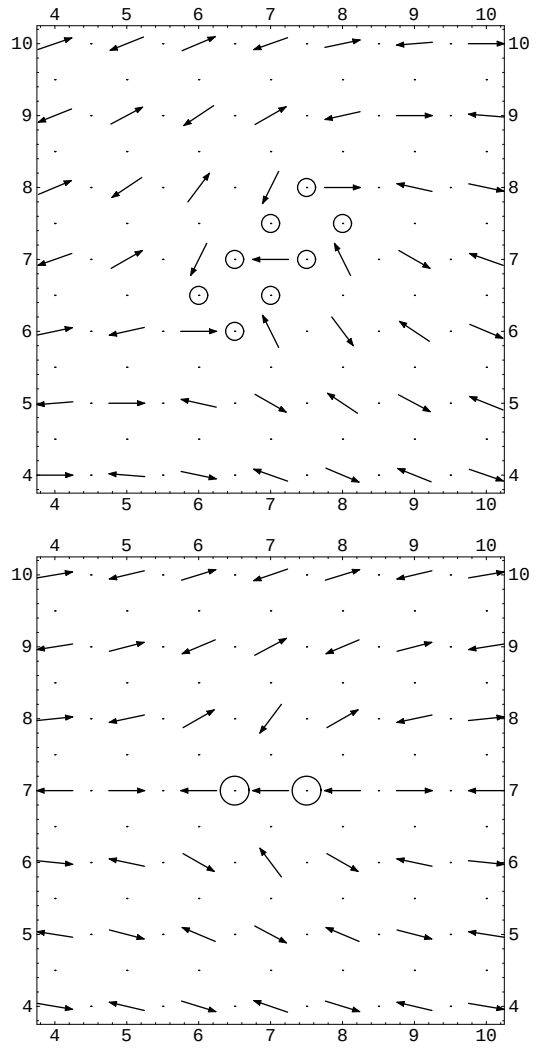


FIG. 5: Starting configurations for the spin and charge density for a system with two holes on a 14×14 lattice: (top) plaquette-centered meron-antimeron pair and (bottom) bond-centered meron-antimeron pair.

IV. CONCLUSIONS

In this paper we have used unconstrained Hartree-Fock theory at $T = 0$, keeping all local spin and charge degrees of freedom to study inhomogenous spin textures in the three-band and the one-band Hubbard model. This approach neglects flucutations around the mean-field solutions. Thus one has to consider the reliability of the these solutions. The HFA predicts the correct behavior for large U_d in the half-filled case. For one doped hole spin polarons are obtained as solutions for the three-band Hubbard model. This agrees with the case of the one-band model [8], in agreement with the mapping [21, 23] of the three-band on the one-band model at low energies. However, we find that in the one-band model an on-site interaction U of the order of the three-band interaction U_d is required to obtain similar results.

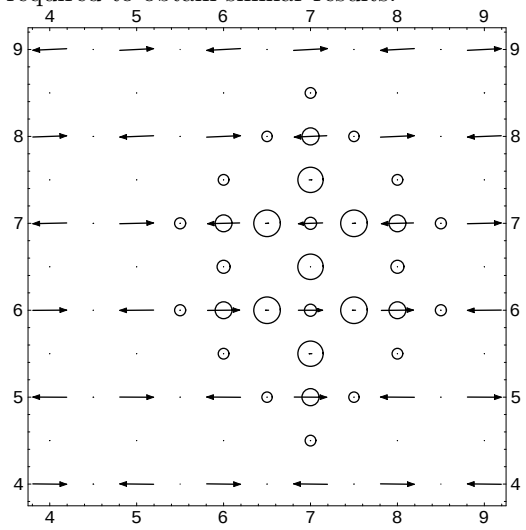


FIG. 6: Resulting double-polaron configuration for two holes on a 14×14 lattice with periodic boundary conditions using the parameters in Eq. (11).

A meron is only a *metastable* self-consistent solution due to its nonzero winding number. As our main result we find that meron-antimeron pairs are not stable solutions in the HFA of the three-band Hubbard model. This holds for periodic as well as open boundary conditions. The same is true for the one-band model. Thus a consistent picture of the one- and three-band models emerges, at least in the framework of the HFA: Both show the same qualitative behavior for weak hole doping.

While the mean-field approximation serves as an useful tool for studying the local charge and spin density, it yields only an upper bound for the true ground-state energy. In the one-band Hubbard model Seibold [9] found a meron-antimeron ground state for $T = 0$ for suitable parameters using a slave-boson method. This method uses a Hartree-Fock ansatz as the initial configuration but treats the spin and charge excitations at each site as distinct bosonic degrees of freedom. It leads to a lower ground state energy than the HFA and is thus the superior variational method. We suggest that this method applied to the repulsive three-band Hubbard model could clarify the still open question of stable meron-antimeron pairs as the effect of hole doping.

[1] A. Aharony, R. J. Birgeneau, A. Coniglio, M. A. Kastner, and H. E. Stanley, Phys. Rev. Lett. **60**, 1330 (1988).

[2] C. Timm and K.H. Bennemann, Phys. Rev. Lett. **84**, 4994 (2000).

[3] F. Krüger and S. Scheidl, Phys. Rev. B **65**, 224502 (2002).

[4] M. Hücker, V. Kataev, J. Pommer, J. Harraß, A. Hosni, C. Pflitsch, R. Gross, and B. Büchner, Phys. Rev. B **59**, R725 (1999).

[5] O. P. Vajk, P. K. Mang, M. Greven, P. M. Gehring, and J. W. Lynn, Science **295**, 1691 (2002).

[6] K. Kato, S. Todo, K. Harada, N. Kawashima, S. Miyashita, and H. Takayama, Phys. Rev. Lett. **84**, 4204 (2000); A. W. Sandvik, Phys. Rev. Lett. **86**, 3209 (2001); Phys. Rev. B **66**, 024418 (2002).

[7] B. I. Shraiman and E. D. Siggia, Phys. Rev. Lett. **61**, 467 (1988).

[8] J. A. Vergés, E. Louis, P. S. Lohmdahl, F. Guinea, and A. R. Bishop, Phys. Rev. B **43**, 6099 (1991).

[9] G. Seibold, E. Sigmund, and V. Hizhnyakov, Phys. Rev. B **57**, 6937 (1998); G. Seibold, Phys. Rev. B **58**, 15520 (1998).

[10] M. Berciu and S. John, Phys. Rev. B **59**, 15143 (1999); *ibid.* **61**, 16454 (2000); Physica B **296**, 143 (2001).

[11] P. B. Wiegmann, Phys. Rev. Lett. **60**, 821 (1988).

[12] R. J. Gooding, Phys. Rev. Lett. **66**, 2266 (1991); R. J. Gooding, N. M. Salem, and A. Mailhot, Phys. Rev. B **49**, 6067 (1994).

[13] E. C. Marino, Phys. Lett. A **263**, 446 (1999); E. C. Marino and M. B. Silva Neto, Phys. Rev. B **64**, 092511 (2001).

[14] J. M. Tranquada, S. J. Sternlieb, J. D. Axe, Y. Nakamura, and S. Uchida, Nature **375**, 561 (1995).

[15] V. J. Emery and S. A. Kivelson, Physica (Amsterdam) **209C**, 597 (1993); Nature **374**, 434 (1995); Phys. Rev. Lett. **74**, 3253 (1995); S. A. Kivelson, E. Fradkin, and V. J. Emery, Nature **393**, 550 (1998).

[16] S. R. White and D. J. Scalapino, Phys. Rev. Lett. **81**, 3227 (1998).

[17] I. Dzyaloshinskii, Phys. Chem. Solids **4**, 241 (1958); T. Moriya, Phys. Rev. **120**, 91 (1960).

[18] D. Coffey, K.S. Bedell, and S.A. Trugman, Phys. Rev. B **42**, 6509 (1990); D. Coffey, T.M. Rice, and F.C. Zhang, *ibid.* **44**, 10112 (1991).

[19] J. A. Vergés, F. Guinea, and E. Louis, Phys. Rev. B **46**, 3562 (1992).

[20] M. P. López Sancho, J. Rubio, M. C. Refolio, and J. M. López Sancho, Phys. Rev. B **46**, 11110 (1992).

[21] F. C. Zhang and T. M. Rice, Phys. Rev. B **37**, 3759 (1988).

[22] J. Zaanen, G. A. Sawatzky, and J. W. Allen, Phys. Rev. Lett. **55**, 418 (1985).

[23] W. Brenig, Phys. Rep. **251**, 153 (1995).

[24] A. Kesting, diploma thesis, Freie Universität Berlin 2002 (unpublished), `http://vwisb7.vkw.tu-dresden.de/~kesting/homepage/diplomarbeit.pdf`.

[25] G. Baumgärtel, J. Schmalian, and K.H. Bennemann, Phys. Rev. B **48**, 3983 (1993).

[26] D. Vaknin, S. K. Sinha, D. E. Moncton, D. C. Johnston, J. M. Newsam, C. R. Safinya, and H. E. King, Jr., Phys. Rev. Lett. **58**, 2802 (1987).

[27] J. R. Schrieffer, X.-G. Wen, and S.-C. Zhang, Phys. Rev. Lett. **60**, 944 (1988).

[28] W. P. Su and X. Y. Chen, Phys. Rev. B **38**, 8879 (1988).

[29] This is the energy needed to add a hole to the half-filled system. First, one has to lift an electron to the Fermi-level which is given by the half of the Mott-Hubbard gap. A second contribution comes from the change of the configuration energy due to the interaction of the particles in the system.